Appl. Math. J. Chinese Univ.
2024, 39(3): 381-397

A new model of flow over stretching (shrinking) and porous sheet with its numerical solutions

Azhar Ali[1,*] Dil Nawaz Khan Marwat[1] Saleem Asghar[2]

Abstract. The viscous fluid flow and heat transfer over a stretching (shrinking) and porous sheets of nonuniform thickness are investigated in this paper. The modeled problem is presented by utilizing the stretching (shrinking) and porous velocities and variable thickness of the sheet and they are combined in a relation. Consequently, the new problem reproduces the different available forms of flow motion and heat transfer maintained over a stretching (shrinking) and porous sheet of variable thickness in one go. As a result, the governing equations are embedded in several parameters which can be transformed into classical cases of stretched (shrunk) flows over porous sheets. A set of general, unusual and new variables is formed to simplify the governing partial differential equations and boundary conditions. The final equations are compared with the classical models to get the validity of the current simulations and they are exactly matched with each other for different choices of parameters of the current problem when their values are properly adjusted and manipulated. Moreover, we have recovered the classical results for special and appropriate values of the parameters (δ_1, δ_2, δ_3, c, and B). The individual and combined effects of all inputs from the boundary are seen on flow and heat transfer properties with the help of a numerical method and the results are compared with classical solutions in special cases. It is noteworthy that the problem describes and enhances the behavior of all field quantities in view of the governing parameters. Numerical result shows that the dual solutions can be found for different possible values of the shrinking parameter. A stability analysis is accomplished and apprehended in order to establish a criterion for the determinations of linearly stable and physically compatible solutions. The significant features and diversity of the modeled equations are scrutinized by recovering the previous problems of fluid flow and heat transfer from a uniformly heated sheet of variable (uniform) thickness with variable (uniform) stretching/shrinking and injection/suction velocities.

Received: 2018-10-20. Revised: 2020-12-05.
MR Subject Classification: 76Dxx, 76D05, 76Mxx, 76M45.
Keywords: permeable stretching (shrinking) sheets, sheet of variable thickness, heat transfer, numerical (dual) solutions, stability analysis.
Digital Object Identifier(DOI): https://doi.org/10.1007/s11766-024-3648-0.
*Corresponding author.

§1 Introduction

Fluid flows and heat transfer over-stretching surfaces have applications in engineering, physics and other fields of science. The experimental investigations which exactly satisfy the theoretical studies of the physical phenomena can be found in [1]. The first paper appeared regarding fluid flows due to stretching surfaces was presented by Sakiadis [2]. Later on, this work was further verified and extended by Tsou et al. [3] and the theoretical results are closely matched with the experimental data. An exact solution of flows due to linear stretching is guaranteed by Crane [4] and further this model is equipped with mass suction (injection) at sheet surface see Gupta [5]. The stretching problem is presented with certain generalizing factors and the modified approach can be found in Kuiken [6]. A 3-D flow induced by horizontally stretched surfaces was examined by Wang [7]. He produced the numerical solution of the transformed boundary values ODE's. The study of stretching (shrinking) flows is further extended and heat transfer effects are included in the previous models. The closed form exact solutions of viscous fluid flows over a permeable and stretching surface (sheets) are discussed in Magyari, and Keller [8]. Later on, an exponential stretching of a rapid decay type was introduced and the results may be seen in Magyari [9]. Further, the models of flows due to stretching were modified by Liao [10], Miklavcic and Wang [11] and different physical cases have been derived when fluid is stretched toward a slit. In Liao [12] multiple solutions were discussed for boundary-layer flows on a stretching flat plate. The flow models of stretching surfaces are modified and generalized by considering different geometries of the surfaces and imposing different physical and mathematically liable conditions and all these models have been discussed through numerical solutions[13-14]. More recently, a paper was published by Zaimi [15] concerning the numerical solution of viscous flow and convective heat transfer on permeable stretching (shrinking) flat plate. Buoyancy effects in boundary layer adjacent to a continuous, moving horizontal flat plate were analyzed by Chen [17]. In his work, he studied the buoyancy-induced stream wise pressure gradient on the momentum and heat transfer characteristics in laminar boundary layer flow adjacent to a continuous, moving horizontal flat plate. It is necessary to study the thermal boundary layer on a continuously semi-infinite moving flat plate. Such a phenomenon has been studied without considering the viscous dissipation effect on taking into account the variable temperature, by Soundalgekar [18]. A scale analysis approach to the correlation of continuous moving sheet (backward boundary layer) forced convective heat transfer, proposed by Jacobi [19]. A problem of boundary layer flow and heat transfer in a quiescent fluid drawing by a power law stretched surface subject to suction or injection was analyzed with its similar solutions by Ali [20]. An analysis was made to study boundary layer flow and heat transfer over an exponentially shrinking sheet by Bhattacharyya [21]. The analysis of Bhattacharyya [21] revealed the conditions for the existence of steady boundary layer flow due to exponential shrinking of the sheet and also investigated that when the mass suction parameter exceeds a certain critical value, steady flow is possible. Due to other engineering applications, unsteadiness is also an integral part of such problems. For this purpose the unsteady mixed convection

boundary layer flow and heat transfer due to a stretching vertical surface in a quiescent viscous and incompressible fluid were studied theoretically by Ishak [22].

Most of the solutions presented in the papers included in the reference list are the numerical solutions of the Navier-Stokes equations. Moreover, these numerical solutions of the Navier-Stokes equations are obtained by transforming them into a system of boundary values ODE's with the appropriate similarity variables. In addition, dual solutions of some classical problems have been obtained, however, we emphasize on the stability of these dual solutions. In order to get the objectives and valid results, it is necessary to consider the unsteady form of the steady flow problem (see [23-28]). A set of common and usual similarity transformations are used in all these papers included in the reference list. As a result, the final boundary values ODE's are obtained in view of the techniques which are solved numerically.

In real engineering systems, the conduction resistance of sheets is necessarily important, whereas, in typical analysis very thin walls are undertaken. The surface thickness is ignored in the classical studies of flow and heat transfer problems. However, it's the compulsory component in many physical problems, therefore, we thoroughly examined the perceptiveness of wall thickness on the field variables and the transport of heat between solid surfaces and fluids. The phenomenon of variable wall thickness is extensively investigated with the combination of other boundary inputs. In this paper, we introduce an interesting and mathematically compact, new and generalized similarity transformation for stream function and similarity variable and hence present the most modified form of transformations. These transformations are used to simplify the boundary value partial differential equations and provide an exact boundary value ODE. Further, these transformations give rise to a new set of parameters that play a role in controlling the suction (injection), stretching (shrinking) and the thickness of the sheet (boundary deformation). Realistic and noticeable features of the study are elaborated by considering the results of the classical models included in the reference list and all these papers are recovered in one go. The final problem (ODE with BCs) is solved by using a numerical method discussed in Cebeci, and Keller [29]. We also present the code and flow chart of the numerical scheme used for the numerical solution of the final third order, nonlinear ODE, which satisfies the boundary condition. This code was developed by Kierzenka and Shampine [30] for solutions of BVPs of ODEs and many problems of two-point BVPs are solved by using these techniques.The effects of different parameters are seen on velocity, temperature and shear stress profiles. Strictly speaking, the set of different profiles includes the cases of Magyari, and Keller [8], Fang [13], Zaimi [15] Bhattacharyya [21] and Ishaq [27] and obviously recovered from the solution of the current model in a special case. Multiple (dual) solutions of the final problem are focused and presented in different graphs and tables. We also found that the dual solution only exists for a certain range of the suction/injection parameters . A linear stability analysis of the dual solutions is focused and presented; however, it is discussed in view of the already established methodology of [23-28]. To the best of our knowledge, this generalized problem has not been studied earlier; therefore, the results obtained are new and different from the classical solutions. The multiple solutions of Magyari, and Keller [8], Zaimi [15], Bhattacharyya [21] and Ishaq [27]

are also extracted from the current model when parameters are fixed accordingly.

§2 Formulation and the numerical solution of the problem

Viscous fluid flow over heated, stretching (shrinking) and permeable surfaces of variable thickness are considered. The continuity, momentum and energy equations subject to the kinematic boundary conditions at the surface of the sheet are given below: The equation of continuity comes from the conservation of mass law, whereas, for incompressible and two dimensional flows it has the following form:

$$\frac{\partial u}{\partial x}+\frac{\partial u}{\partial y}=0 \tag{1}$$

The following momentum equation comes from the Newton's second law of motion, however, it is the steady, two dimensional and boundary layer form of the Navier Stokes equation and valid for laminar flow of fluid, which has uniform viscosity:

$$u\frac{\partial u}{\partial x}+v\frac{\partial u}{\partial y}=\nu\frac{\partial^2 u}{\partial y^2} \tag{2}$$

The energy equation comes from the first law of thermodynamics and the boundary layer form of this equation is presented below and it is valid for the fluids of uninform thermal properties without the viscous dissipation term:

$$u\frac{\partial T}{\partial x}+v\frac{\partial T}{\partial y}=\frac{\kappa}{\rho c_p}\frac{\partial^2 T}{\partial y^2} \tag{3}$$

The velocity field has two components; $u(x,y)$ and $v(x,y)$ in x and y directions, respectively. Further, T, $\nu=\frac{\mu}{\rho}$, κ and c_p are temperature, kinematic viscosity, density, thermal conductivity and specific heat respectively. The kinematic viscosity ($\nu=\mu/\rho$), coefficient of fluid viscosity (μ) and density (ρ) are constants in the flow region. Boundary conditions for the momentum equation are described below:

$$u(x,y)=U_w(x),\ v(x,y)=V_w(x)\ \text{ at }\ y=f(x), \tag{4}$$

$$u(x,y)=U_\infty(x)=0, \tag{5}$$

The sheets are assumed of very small thickness in the classical simulations of flow over a plate. However, the thickness of the sheets is of significant importance in the practical problems of heat transfer from the surface of wall into the fluid. Therefore, we have taken the sheet of nonuniform thickness in the current analysis. Here we have taken the boundary layer flow over a heated, porous and stretching/ shrinking sheet of variable thickness so it is mandatory that the fluid in contact with sheet will have the temperature of the sheet due to no temperature jump condition. Moreover, the stagnant fluid away from the sheet has an ambient temperature. Note that here we only considered the case of heat transfer at the surface of the sheet and this is the reason that the following physical conditions are taken for temperature at the surface of the sheet:

$$T=T_w\ \text{ at }\ y=A\sqrt{d}\alpha^{\beta},\ \ T=T_\infty\ \text{ when }\ y\to\infty, \tag{6}$$

Note that $f(x)=A\sqrt{d}\alpha^{\beta}$, $\alpha=d_0+(d_1+2d_2)A_1x$ and $\beta=\frac{d_1+d_2}{d_1+2d_2}$. Also $U_w(x)=\frac{B}{d_2}A_2\alpha^{1-2\beta}$ and $V_w(x)=\frac{c}{\sqrt{d_2}}A_1A_2\alpha^{-\beta}$ are stretching (shrinking) and injection (suction) velocities, re-

spectively. Further, $V_w \succ 0 (U_w \succ 0)$ for injection (stretching), $V_w \prec 0 (U_w \prec 0)$ for suction (shrinking) and $V_w = 0 (U_w = 0)$ correspond to an impermeable (fixed) sheet. Further, A, A_1, A_2, B, c, d_0, d_1 and d_2 are the controlling parameters. Note that $T_w = T_\infty + T_0(\frac{\alpha}{A_1})^{k_1/\tau}$ is the variable temperature of the sheet, T_∞ is the constant free stream temperature, where $\tau = d_1 + 2d_2$ and T_0 and $k_1 (k_1 = -d_1)$ are constant temperature controlling parameters.

The concept of stream function for two dimensional flow is the great obligation of Stokes, therefore, it is also known as the Stokes stream function. The stream function of two variables give arbitrary lines/ curves in the flow field and its derivatives with respect to each of these variables gives the velocity components. Note that the two variables usually representing the Cartesian Coordinates in two dimensional plane. We may get rid of the continuity equation (1) by invoking the proper definition of the stream function. On the other hand, Blasius used the stream function for simplifying the viscous flow model maintained over a sheet and introduced the similarity variables such that the governing partial differential equations of continuity and boundary layer form of momentum equation are transformed into a single ODE. The following similarity transformations are introduced in terms of stream functions ψ, temperature T and similarity variable η:

$$\psi = A_2 \frac{\alpha^{1-\beta}}{\sqrt{d_2}} f(\eta), \quad \theta(\eta) = \frac{T - T_\infty}{T_w - T_\infty}, \quad \eta = \frac{y}{\sqrt{d_2}} \alpha^{-\beta}, \tag{7}$$

where η is the similarity variable and $f(\eta)$ and $\theta(\eta)$ are unknown functions, representing velocity components and temperature respectively. The stream function satisfies the relations $u = \frac{\partial \psi}{\partial y}$ and $v = -\frac{\partial \psi}{\partial x}$. In view of these definitions, Eq. (1) is identically satisfied and by substituting the transformations defined in Eq. (7) into Eqs. (2-5), we obtain the following exact boundary value ODE:

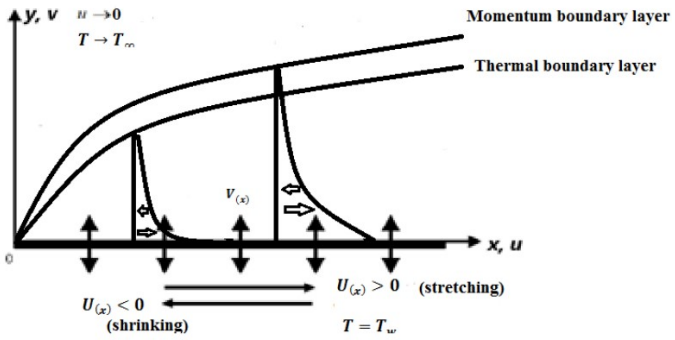

Figure 1. Physical geometry of the problem.

$$f''' + \delta_1 f'^2 + \delta_2 f f'' = 0, \tag{8}$$

$$\theta'' + Pr\,(\delta_2 f \theta' - \delta_3 f' \theta) = 0, \tag{9}$$

$$f(A) = \frac{-c + AB(d_1 + d_2)}{d_2}, \quad f'(A) + b, \quad f'(\infty) = 0, \tag{10}$$

$$\theta(A) = 1, \quad \theta(\infty) = 0, \tag{11}$$

where $\delta_1 = \frac{A_1 A_2 d_1}{\nu}$, $\delta_2 = \frac{A_1 A_2 d_2}{\nu}$, $\delta_3 = \frac{A_1 A_2 k_1}{\nu}$, $Pr = \frac{\nu}{\alpha}$ and A_2, $k_1 (k_1 = -d_1)$ are constant temperature controlling parameters. Note that δ_1 and δ_2 determine the non-linear nature of stretching (shrinking) and injection (suction) velocities, respectively, whereas, δ_3 determines the non-linearity in the variable temperature of the sheet.

§3 Flwo chart for MATLAB Script *bvp4c*

The nonlinear boundary value problem in equations (8-11) is solved numerically with the help of the numerical scheme developed by Cebeci and Keller [29]. In this section, we present the code and flow chart for the employed numerical scheme for the numerical solution of the final third order, nonlinear ODE's (8-9), satisfying the boundary conditions (10-11). There are built-in functions in MATLAB which can solve BVPs and the two very famous and advantageous methos i.e. *bvp4c* and *bvp5c* are widely used for the solution of such problems. These techniques are residual control based and adoptive mesh solvers. These codes were developed by Kierzenka and Shampine [30] for solutions of BVPs of ODEs and many problems of two-point BVPs are solved by using these techniques. The MATLAB package bvp4c integrates the system of ODEs in Eqs. (8-9) on the interval [A, S] subject to two-point boundary value conditions given in Eqs. (10-11) where S represents the lab infinity. This technique gives a continuous solution to the problem on [A, S]. This method requires reducing the system of third and second-order ODEs into five first-order systems of ODEs. It is a finite difference scheme based on a three-stage Lobatoo IIIa collocation technique and the collocation polynomial gives a fourth-order accurate solution which is uniformly changed on [A, S]. A convergent solution is found for the minimum number of initial mesh points, which are 5. The mesh size and error minimization strictly depend upon the residual of the solution.

The system of BVPs in Eqs. (8-11) is solved by *bvp4c* which contains two unknown functions f and θ. The MATLAB code is used to solve the problem numerically. The script file employed for the solution of the modeled problem does not need external function files for specifying the ODE's and their relevant BCs. The script file will also need an initial guess for the unknown field quantites depending upon the total order of the system of ODE's. The general Matlab script file for the solution of Eqs. (8-9) satisfying the boundary conditons in Eqs. (10-11) is given in the link https://ww2.mathworks.cn/help/matlab/ref/bvp4c.html.

§4 Graphs and their discussion

The nonlinear boundary value problem in equations (8 - 11) is solved numerically with the help of the numerical scheme developed by Cebeci and Keller [29]. The modeled equations are also compared with the classical simulations for special values of the controlling parameters. Effects of different parameters are seen on the velocity, temperature and shear stress profiles. In one case, the dual solutions of velocity profiles are also presented and further investigations of

all such solutions have been elaborated in the following consequent subsections. Note that the effects of different parameters are seen in different graphs and tables and thoroughly discussed in the following sections. For sake of simplicity and convenience, we divide this section into four subsections.

4.1 Comparison of the solutions with the classical results:

The nonlinear boundary value problem in equations (8 - 11) is solved numerically with the help of the numerical scheme developed by Cebeci and Keller [29]. Moreover, we retrieved the published results for the specific values of the parameters of the current model. Initially, the problem in [13] is recovered when special values are proposed for the involved parameters in the problem in equations (8 - 11)(*i.e.* $A = 0,\ B = -1,\ c = -s,\ \delta_1 = -\beta,\ \delta_2 = d_2 = 1$, where the symbols β & s represent the controlling and injection/ suction parameters, respectively in [13]). The results obtained for the special values are shown in Figs. 2-3, whereas the profiles shown in the plots are the replicate of the solutions in [13]. We also retrieved the model published in [8] for the parameters value: $A = 0,\ \delta_1 = -2m/(m+1),\ for\ m = -1/3,\ \delta_2 = d_2 = 1,\ B = 1$ and $c = -f_w$. These numerical values of the parameters exactly provided the same set of problems as discussed in [8]. Note that m is the representative of f_w where m is any finite real number used in [8]. They provide the exact solution to the model equations for a special value of parameters. In [8], only exact solutions of the problem are discussed. The comparison of the current model with [8] ensures the validity and authenticity of the formulation and its numerical solutions. These numerical solutions are shown in Figs.4-5. On the other hand, the modeled problem that appeared in [15] is also a special case of the current model when we provide values to the parameters as $A = 0,\ \delta_1 = -1,\ \delta_2 = d_1 = d_2 = 1,\ B = \sigma = -0.2$ and $c = -S$. Where σ & S are responsible for stretching/ shrinking and suction/ injection in [15]. The observations are recorded in Fig. 6 and the solutions are exactly matched with the results of [15]. These arguments have confirmed the validity of the current model.

4.2 Velocity profiles

Numerical solutions of the modeled problem in equations (8) and (10) are presented for the components of velocity and multiple results are obtained for different parameters value. The axial velocity component (f') is graphed in Fig. 2 for different δ_1. A thin boundary layer is seen near the sheet for small values δ_1 and $c \prec 0$. In Fig. 3, effects $c \prec 0$ are noted on the velocity profiles and massive flow overshoot is seen near the surface. The variation in parameters caused changes in downstream velocity. As a result, an abrupt and maximum increase in the velocity is observed in Figs. 4-5 with simultaneous changes in the permeable stretching sheet. In these figures, the velocity profiles have high peaks for c and B. Therefore, as c decreases from $+\infty$ to $-\infty$, the shape of velocity profiles *at* the wall changes from convex to concave as the value $c = 1$ is reached. For $1 \succ c \succ -1$ the shape of the velocity profiles near the wall is still concave, whereas, for $c \prec 1$ once again they become convex. As one switches from injection ($c \succ 1$)

to suction ($c \prec 1$) and it obviously implies a change from positive to negative skin friction, therefore, a sudden increase in the velocity profiles with peaks is observed. For large c and $B \succ 0$, high peaks of the velocity profiles are observed which are shown in Fig. 6. Note that the velocity of the fluid is retarded (in the absolute sense) and the boundary layer is increased with the increasing of while significant changes in the behavior of the boundary layer have been seen. Effects of the different parameters on fluid velocity ($f'(\eta)$) are observed inside the boundary layer. More results for the velocity profiles are also shown in Figs.7-8 for different A and fixed $c \prec 0$. In these observations, negative and positive values are taken for A and the results are shown in Figs. 7-8, respectively. In Fig. 7, $f'(\eta)$ profiles are increased with the decreasing of $A(\prec 0)$. Contrary to that, in Fig. 8, $f'(\eta)$ is decreased when A is increasing and the boundary layers thickness is also increased. On the other hand, the graphs are changing their position around the origin with the variation in A depending upon its sign. These types of changes in profiles are related to translation of the graphs on η-axis by A. In Fig. 9, the decreasing behavior of fluid velocity and boundary layers against the increasing B is noted. Whereas in Fig. 10 effects of $B \prec 0$ are studied on fluid velocity. The fluid velocity is decreased and boundary layer thickness is increased with the decreasing of B.

4.3 Shear stress profiles

Here we present the shear stress profiles which obtained from the solution of equations (8) and (10). The shear stress profiles are consistently graphed in Figs. 2-3 and Figs. 7-10 in order to discuss the behavior of shear stress profiles for the current model against different parameters subject to the classical data. It is a fact that the current formulation includes the modeling of power law stretching. More precisely, the published profiles for (f'') are recovered from the current model and shown in Figs. 2-3 for different δ_1. In view of these observations, the influence of all parameters is observed on $f''(\eta)$. Besides that, the wall drag is increased with decreasing of δ_1. More classical results are also recovered for $f''(\eta)$ from the current problems and shown in Figs. 7-8. These two graphs are plotted for different A (surface deformation) and $c \prec 0$ (suction case). The analysis is further extended for negative and positive values of A and the results are shown in Figs. 7-8, respectively. In Fig. 7, $f''(\eta)$ is increased with the decreasing of $A(A \prec 0)$. Whereas, in Fig. 8, the profiles of $f''(\eta)$ are decreased with the increasing values of A. Moreover, profiles are translated backward (forward) from the origin according to A if taken negative (positive). The variation in A, just shifts the profiles to the left or right side of η-axis by the value of $A(A \succ 0)$. Figs. 9-10 show the graphs of $f''(\eta)$ for different values of $B \succ 0$ (stretching) and $B \prec 0$ (shrinking), respectively. In Fig. 9 shear stress is decreased with the increasing of B. In Fig. 10 effects of $B \prec 0$ are analyzed on f'' and it is increased with decreasing B.

In Table 1, the quantitative results of skin friction coefficient $f''(0)$ is presented and compared with [4], [15] and [30]. The skin friction coefficient is decreases as the magnitude ofn the stretching/shrinking parameter increases in the absence of suction or injection. A good

agreement between the results is found as shown in this table. Similarly in Table 2 comparison of $\theta'(0)$ is made with [26-29]. Results in this table are matched to the best accuracy level. We conclude from this table that an increase in Pr leads to an increase in the amount of heat transfer at the surface of the sheet.

Table 1. $f''(0)$ is compared with existing literature when $A = 0,\ \delta_1 = -1$ and $d_1 = d_2 = \delta_2 = 1$.

Different B, $c = 0$	Results in [4]	Results in [15]	Results in [22]	New Results
0.1	-	-0.031623	-	-0.03164
0.5	-	-0.353553	-	-0.35355
1	-1	-1.000000	-1.000000	-1.000000
2	-	-2.828427	-	-2.82843

Table 2. $\theta'(0)$ is compared with existing literature when $A = c = d_1 = \delta_1 = 0,\ B = \delta_2 = \delta_3 = d_2 = 1$ and different Pr.

Pr	Results in [3]	Results in [17]	Results in [18]	Results in [19]	Results in [20]	New results
0.7	0.3492	0.34924	0.3508	0.3492	0.3476	0.34927
0.1	0.4438	-	-	0.4438	0.4416	0.44375
10.0	1.6804	-	1.6808	1.6790	1.6713	1.68031

4.4 Dual solutions of the problem

In this section, we are emphasize on the dual solution of the modeled problem in equations (8) and (10). Dual solutions of the unknown function f' are found for the same set of parameters value and the velocity is graphed in Fig.6. There are two branches of profiles in this figure and groups are named by "**First solution**" and "**Second solution**". It is observed from the "**First solution**" group that the absolute velocity of the fluid is decreased when c is increasing. It is concluded that the suction retards the flow. Moreover, it is also confirmed that the boundary layer size is minimized with the increasing of c and the opposite behavior of the velocity is recorded in the "**Second solution**" group. In the "**Second solution**" group the boundary layer size is propagated when c is increasing and significant changes have been noted in it. For the sake of convenience, we avoided more dual solutions of the model problem obtained for other sets of parameter values.

In Fig 11, dual temperature profiles $\theta(\eta)$ are demonstrated for different values of c. In first solution, there is a fall or decrease in the temperature of the fluid with the increasing of c, however, these profiles in the second solution are increased with the increasing of c for fixed values of Pr and similar predictions/results are reported in [21]. Besides that, the order of the thermal boundary layer is smaller in the case of the first solution as compared to the order of the boundary layer in the second solution.

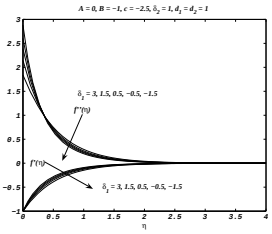

Figure 2. Variation in the profiles of f' and f'' against η for different δ_1 and compared with [13].

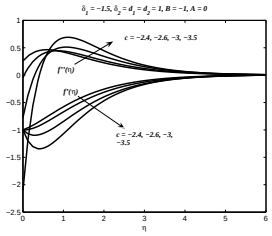

Figure 3. Variation in the profiles of f' and f'' against η for different $c \prec 0$ and compared with [13].

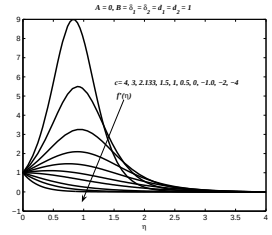

Figure 4. Variation in the profiles of f' against η for different $c \succ 0 (c \prec 0)$ and compared with [8].

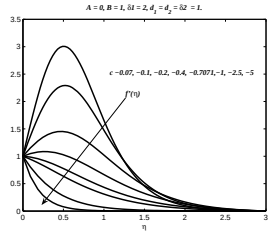

Figure 5. Variation in the profiles of f' against η for different $c \prec 0$ and compared with [8].

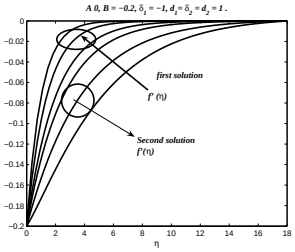

Figure 6. Variation in the profiles of f' against η (Dual solutions) for different $c \prec 0$ and compared with [15].

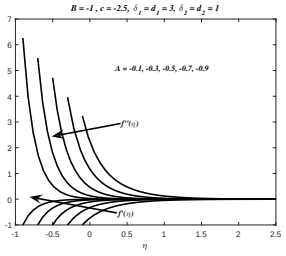

Figure 7. Variation in the profiles of f' and f'' against η for different $A(\prec 0)$.

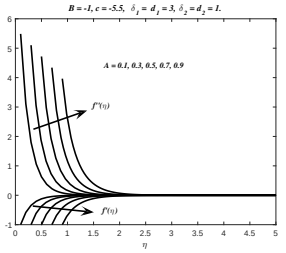

Figure 8. Variation in the profiles of f' and f'' against η for different $A(\succ 0)$.

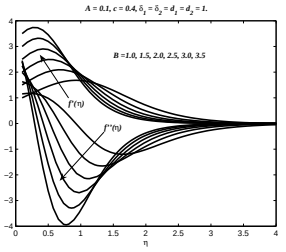

Figure 9. Variation in the profiles of f' and f'' against η for different $B(\succ 0)$.

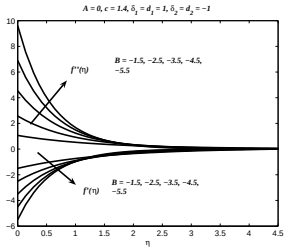

Figure 10. Variation in the profiles of f' and f'' against η for different $B(\prec 0)$.

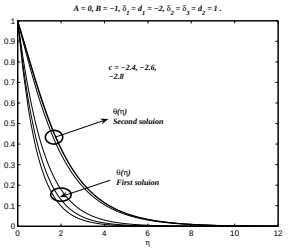

Figure 11. Dual solutions of $\theta(\eta)$ (PST) are plotted for different c, $(B \prec 0)$ and match with [21].

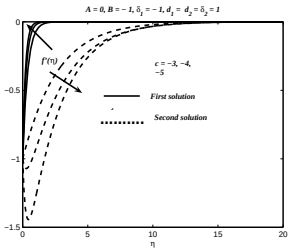

Figure 12. Variations in the profiles of f' against η (Dual solutions) for $c \prec 0$ and compared with [27].

§5 Stability analysis of solutions

The dual solutions of equations (8-11) are presented in Figs. 6, 11 & 12 for shrinking sheet and wide range of suction/injection parameter c. However, we are searching for the stability of these two solutions. Therefore, it is important to consider the unsteady form of equations of motion (1 & 2) and note that equation (1) is valid for both steady and unsteady flows whereas equation (2) is replaced by:

$$\frac{\partial u}{\partial t} + u\frac{\partial u}{\partial x} + v\frac{\partial u}{\partial y} = \nu\frac{\partial^2 u}{\partial y^2}, \tag{12}$$

where t denotes the time variable. Keeping in view equation (7), we introduce the following new dimensionless variable for the stream function and similarity variable

$$\psi = A_2 \frac{\alpha^{1-\beta}}{\sqrt{d_2}} f(\eta), \quad \eta = \frac{y}{\sqrt{d_2}} \alpha^{-\beta}, \quad \tau = at. \tag{13}$$

Note that the variable τ gives rise to an initial value problem and meanwhile, it is consistent with the practical solutions that we may have. We hope that the stability of the first (upper) and second (lower) branches solutions for a general time-dependent problem is directly associated with steady states stable and unstable problems, respectively see [23]. By invoking the assertions for the steam function and similarity variables in equation (13) into equation (12) we obtained that:

$$\frac{\partial^3 f}{\partial \eta^3} + \delta_2 \left(f \frac{\partial^2 f}{\partial \eta^2} - \left(\frac{\partial f}{\partial \eta} \right)^2 \right) - \delta_4 \frac{\partial^2 f}{\partial \eta \partial \tau} = 0, \tag{14}$$

Subject to the boundary conditions:

$$f(A, \tau) = \frac{-c + AB(d_1 + d_2)}{d_2}, \quad \frac{\partial f}{\partial \eta}(A, \tau) = B, \quad \frac{\partial f}{\partial \eta}(\infty, \tau) = 0, \tag{15}$$

where $\delta_4 = ad_2/\nu$. Note that equation (14) is similar by taking the assumption $\delta_1 = -\delta_2$. The stability of the solution of steady flow problem can be obtained by a well-established and standard method. Finally, we established the methodology of [23-28] and decomposed the solution of Eq. (14) as under:

$$f(\eta, \tau) = f_0(\eta) + e^{-\gamma \tau} F(\eta, \tau), \tag{16}$$

where the first component in Eq. (16) *i.e.* $f(\eta) = f_0(\eta)$ satisfies the boundary value problem in equations (8) and (10), and γ represents an unknown eigenvalue. Moreover, the unknown function $F(\eta, \tau)$ in the second component of Eq. (16) is asymptotically smaller than $f_0(\eta)$. On the other hand, the problem in equations (14-15) contains eigenvalues and by Strum-Liouville theorem there exists an infinite number of eigenvalues such that $\gamma_1 \prec \gamma_2 \prec \cdots$. If the smallest eigenvalue is negative then the solution in Eq. (16) grows exponentially and the flow remains unstable due to these disturbances. However, the solution in Eq. (16) decays exponentially for the largest positive eigenvalues and the flow becomes stable in this case. Substituting equation (16) into equation (14), we obtain the following linearized problem.

$$\frac{\partial^3 F}{\partial \eta^3} + \delta_2 f_0 \frac{\partial^2 F}{\partial \eta^2} + \delta_2 F f_0'' + (\gamma \delta_4 - 2\delta_2 f_0') \frac{\partial F}{\partial \eta} + \frac{\partial^2 F}{\partial \eta \partial \tau}, \tag{17}$$

with the boundary conditions

$$F(0, \tau) = 0, \quad \frac{\partial F}{\partial \eta}(0, \tau) = 0, \quad \frac{\partial F}{\partial \eta}(\eta, \tau) \to 0 \quad \text{as} \quad \eta \to \infty. \tag{18}$$

In fact, the significant observation and analysis of [23] are still valid for the current simulations when $\gamma = 0$ and $\delta_1 = -\delta_2$ whereas the problem in equations (17-18) is homogenous. The solution $f(\eta) = f_0(\eta)$ of the steady boundary value problem in equations (8) and (10) may be obtained by setting $\tau = 0$ and $\delta_1 = -\delta_2$. Hence, the unknown function $F(\eta) = F_0(\eta)$ in equation (17) is associated with the initial growth or decay of the solution (16). In this regard we have to solve the following linear eigenvalue problem:

$$F_0''' + \delta_2 f_0 F_0'' + (\gamma \delta_4 - 2\delta_2 f_0') F_0' = 0. \tag{19}$$

With the boundary conditions

$$F_0(0) = 0, \quad F_0'(0) = 0, \quad F_0'(\infty) = 0. \tag{20}$$

The stability of the corresponding steady flow solution $f_0(\eta)$ will be determined by the smallest eigenvalue γ. A feasible region for finding the eigenvalue can be selected by adjusting the condition on $F_0(\eta)$ see [28]. A new boundary condition will be imposed in order to determine an eigenvalue from the solution of Eqs. (19-20) for a certain initial fixed value of γ. We solved the problem in equations (19-20) with the additional boundary condition $F_0''(0) = 1$. In addition, unique solutions of Eqs. (8) and (10) are obtained for stretching cases whereas the dual solutions are found for flow over a shrinking sheet.

The existence of dual solutions was reported in [11] for shrinking sheet problems and Figs. 6 & 12 of equations (8) and (10) provide sufficient arguments for the existence of dual solutions. Notice that these two figures represent the unknown velocity function f' and are graphed for shrinking cases in terms of different non-zero values of suction parameter c. The stability analysis of these solutions is established by finding the eigenvalue γ involved in equation (16). The smallest eigenvalues γ are presented in Table 3 for fixed values of suction parameter c which shows that γ is positive for the first (upper branch) solution and negative for the second (lower branch) solution. Thus, we assert that the first (upper branches) solution is linearly stable and physically acceptable, while the second (lower branches) solution is linearly unstable when $\delta_1 = -1,\ \delta_2 = 1,\ A = 0$ and $B = -0.2$ or $B = -1$. A comparative analysis is given in Fig. 12 and Table 3 and new results are compared with the previous results of [27] for $\delta_1 = -1,\ \delta_2 = 1,\ A = 0$ and $B = -1$ which supports the validity of the numerical solution of the modeled problem and its stability analysis with the best accuracy.

Table 3. The smallest eigenvalues γ for $\delta_1 = -1$ and $\delta_2 = 1$ and compared with [27].

	First (Upper Branch) Solution		First (Lower Branch) Solution	
$(c,\ B)$	Present	Previous [27]	Present	Previous [27]
$(-0.9, -0.2)$	0.063	-	-0.058	-
$(-1.0, -0.2)$	0.166	-	-0.135	-
$(-1.2, -0.2)$	0.315	-	-0.224	-
$(-2.1, -1)$	0.404	0.4040	-0.336	-0.3355
$(-2.3, -1)$	0.757	0.7574	-0.537	-0.5371
$(-2.5, -1)$	1.053	1.0527	-0.652	-0.6511
$(-3, -1)$	1.795	1.7952	-0.805	-0.8042
$(-4, -1)$	3.585	3.5817	-1.198	-0.9514
$(-5, -1)$	5.836	5.7390	-1.489	-1.4885

§6 Conclusion

The classical simulation of flows and heat transfer overheated, thin and uniform sheets are generalized for the fluid flow and heat transfer on the plates of nonuniform thickness with

variable stretching (shrinking) and injection (suction) velocities and nonuniform surface temperature. The current modeled problem is described as the most accurate version of a real engineering system of heat transfer which has variable and plump surfaces. A more realistic model and its solutions are presented to reveal the latest facts regarding viscous fluid flows on a stretching (shrinking) and porous sheet of variable thickness and encompass all the information previously emerged in different published research articles. The problem is formulated in terms of new and unusual transactions for the stream function and obviously invokes the results shown by Magyari and Keller [8], Fang [13], Zaimi [15], Bhattacharyya [21] and Ishaq [27] when parameters of the current article have been properly adjusted. Finally, the effects of all parameters and their physical consequences have been seen on fluid velocity, temperature and shear stress profiles which are concurrent to the previously published results. The numerical results are evidence of the fact that the dual solutions are possible for different values of the shrinking parameter whereas it is not the case for stretching sheet problems. The stability analysis showed that the solution in Eq. (16) decays (grows) for the upper (lower) branch solution. Thus, the first (upper branches) solution is linearly stable, while the second (lower branches) solution is linearly unstable. Note the upper branch solutions correspondg to positive values of eigenvalues and vice versa. The main physical results of the current problem can be summarized as follows.

1. The skin friction coefficient is decreases as the magnitude of the stretching/shrinking parameter increases when $c = 0,\ A = 0,\ \delta_1 = -1,\ d_1 = d_2 = \delta_2 = 1$.

2. The velocity of fluid is retarded (in the absolute sense) and the boundary layer is increased with the increasing of c while significant changes in the behavior of the boundary layers (*i.e.* momentum and thermal boundary layers) have been seen.

3. The rate of heat transfer at the surface increases with the increase of Pr when $A = c = d_1 = \delta_1 = 0$ and $B = \delta_2 = \delta_3 = d_2 = 1$.

Declarations

Conflict of interest The authors declare no conflict of interest.

References

[1] E G Fisher. *Extrusion of Plastics*, Wiley, 1976.

[2] B C Sakiadis. *Boundary-layer behavior on continuous solid surface:II. Boundary-layer on a continuous flat surface*, AIChE Journal, 1961, 7(2): 221-225.

[3] F K Tsou, E M Sparrow, R J Goldstein. *Flow and heat transfer in the boundary layer on a continuous moving surface*, International Journal of Heat and Mass Transfer, 1967, 10(2): 219-235.

[4] L G Crane. *Flow past a stretching plate*, Journal of Applied Mathematics and Physics, 1970, 21: 645-647.

[5] P S Gupta, A S Gupta. *Heat and mass transfer on a stretching sheet with suction or blowing*, The Canadian Journal of Chemical Engineering, 1977, 55(6): 744-746.

[6] H K Kuiken. *On Boundary Layers in Fluid Mechanics that Decay Algebraically along Stretches of Wall that are not Vanishingly Small*, IMA Journal of Applied Mathematicse, 1981, 27(4): 387-405.

[7] C Y Wang. *The three-dimensional flow due to a stretching flat surface*, Phys Fluids, 1984, 27(8): 1915-1917.

[8] E Magyari, B Keller. *Exact solutions for self-similar boundary-layer flows induced by permeable stretching walls*,European Journal of Mechanics-B/Fluids, 2000, 19(1): 109-122.

[9] E Magyari, M E Ali, B Keller. *Heat and mass transfer characteristics of the self-similar boundary-layer flows induced by continuous surfaces stretched with rapidly decreasing velocities*, Heat and Mass Transfer, 2001, 38: 65-74.

[10] L Liao. *A new branch of solutions of boundary-layer flows over an impermeable stretched plate*, International Journal of Heat and Mass Transfer, 2005, 48(12): 2529-2539.

[11] M Miklavcic, C Y Wang. *Viscous Flow due to Shrinking sheet*, Quarterly of Applied Mathematics, 2006, LXIV: 283-290.

[12] S J Liao. *A new branch of solutions of boundary-layer flows over a permeable stretching plate*, International Journal of Non-Linear Mechanics, 2007, 42(6): 819-830.

[13] T F Fang. *Boundary Layer Flow Over a Shrinking Sheet With Power Law Velocity*, International Journal of Heat and Mass Transfer, 2008, 51(25-26): 5838-5843.

[14] K Zaimi, A Ishak, I Pop. *Flow Past a Permeable Stretching/Shrinking Sheet in a Nanofluid Using Two-Phase Model*, PloS One, 2014, 9(11), https://doi.org/10.1371/journal.pone.0111743.

[15] K Zaimi, A Ishak. *Boundary Layer Flow and Heat Transfer over a Permeable Stretching/Shrinking Sheet with a Convective Boundary Condition*, Journal of Applied Fluid Mechanics, 2015, 8(3): 499-505.

[16] H B Keller, T Cebeci. *Accurate numerical methods for boundary layer flows I. Two dimensional laminar flows*, In: Holt, M. (eds) Proceedings of the Second International Conference on Numerical Methods in Fluid Dynamics, Lecture Notes in Physics, Spriger, Berlin, Heidelberg, 1971, 8: 92-100.

[17] T S Chen, F A Strobel. *Buoyancy effects in boundary layer adjacent to a continuous moving horizontal flat plate*, Journal of Heat and Mass Transfer, 1980, 102(1): 170-172.

[18] V M Soundalgekar, T V Ramana Murty. *Heat transfer in flow past a continuous moving plate with variable temperature*, Wärme-und Stoffübertragung, 1980, 14: 91-93.

[19] A M Jacobi. *A scale analysis approach to the correlation of continuous moving sheet (backward boundary layer) forced convective heat transfer*, Journal of Heat and Mass Transfer, 1993, 115(4): 1058-1061.

[20] A E Mohamed. *On thermal boundary layer on a power-law stretched surface with suction or injection*, International Journal of Heat and Fluid Flow, 1995, 16(4): 280-290.

[21] K Bhattacharyya. *Boundary layer flow and heat transfer over an exponentially shrinking sheet*, Chinese Physics Letters, 2011, 28(7), https://doi.org/10.1088/0256-307X/28/7/074701.

[22] A Ishak, R Nazar, I Pop. *Unsteady mixed convection boundary layer flow due to a stretching vertical surface*, Arabian Journal for Science and Engineering, 2006, 31(2): 165-182.

[23] J H Merkin. *Travelling waves in autocatalytic chemical systems with decay: Bounds on existence*, Journal of Engineering Mathematics, 2007, 59(2): 195-206.

[24] P D Weidman, D G Kubitschek, A M J Davis. *The effect of transpiration on self-similar boundary layer flow over moving surfaces*, International Journal of Engineering Science, 2006, 44(11-12): 730-737.

[25] A Postelnicu, I Pop. *Falkner-Skan boundary layer flow of a power-law fluid past a stretching wedge*, Applied Mathematics and Computation, 2011, 217(9): 4359-4368.

[26] A V Roşca, I Pop. *Flow and heat transfer over a vertical permeable stretching/ shrinking sheet with a second order slip*, International Journal of Heat and Mass Transfer, 2013, 60: 355-364.

[27] A Ishak. *Flow and Heat Transfer over a Shrinking Sheet:A Stability Analysis*, World Academy of Science, Engineering and Technology, International Journal of Mechanical, 2014, 8: 902-906.

[28] S D Harris, D B Ingham, I Pop. *Mixed convection boundary-layer flow near the stagnation point on a vertical surface in a porous medium: Brinkman model with slip*, Transport in Porous Media, 2014, 77: 267-285.

[29] T Cebeci, H B Keller. *Shooting and parallel shooting methods for solving the Falkner-Skan boundary-layer equation*, Journal of Computational Physics, 1971, 7(2): 289-300.

[30] J Kierzenka, L F Shampine. *A BVP solver based on residual control and the Maltab PSE*, ACM Transactions on Mathematical Software, 2001, 27(3): 299-316.

[1]Department of Mathematics, Islamia College Peshawar 25120, Jamrod road, Peshawar, Khyber Pakhtunkhwa, Pakistan.

Emails: azhar_ali017@yahoo.com, dnm512@yahoo.com

[2]Department of Mathematics, COMSATS Institute of Information Technology, Park Road, Tarlai Kalan, Islamabad 45550, Pakistan.

Email: sasghar@comsats.edu.pk